Summary of the 2018 Asian Summer Monsoon

1. Precipitation and temperature

CLIMAT report data detailing the four-month mean temperature for the monsoon season (June – September) show anomalies of more than 1°C above the normal from Japan to central China, in the southern part of Central Siberia and across areas in and around western Pakistan, while values of 1°C and below are seen for parts of western China and from southern Myanmar to western Thailand (Figure 11). From June to August in particular, higher-than-normal temperatures have persisted around the mid-latitude band from 25°N to 45°N, with record seasonal mean temperatures in eastern Japan (the highest since 1946), South Korea (1973) and China (1961). New daily maximum temperatures were also recorded in Japan (41.1°C, Kumagaya, July 23) and South Korea (41.0°C, Hongcheon, August 1).

Four-month total precipitation amounts for the same period were more than 140% of the normal in Hokkaido and western regions of Japan, in and around northern China, from western China to northwestern India, in and around southern China, and in and around the western part of New Guinea, but were less than 60% of the normal in southern Pakistan and southeastern Indonesia (Figure 12). In western Japan, multiple landfall typhoons and active seasonal stationary fronts caused anomalous high precipitation amounts from July to September, resulting in the second-highest monthly precipitation amounts for September since 1946 on the Pacific Ocean side of the country.

2. Tropical cyclones

A total of 25 tropical cyclones (TCs[1]) had formed over the western North Pacific up to September 2018 as compared to the normal of 18.4. The total of 9 TCs forming in August was the second-highest since 1951 (Table 1).

From June to September, a total of 5 TCs with maximum sustained wind speeds of more than 105 knots (classified by RSMC Tokyo as Violent typhoons) made landfall on China, Japan, the Philippines and South Korea.

The most intense of these TCs – Typhoon Mangkhut – formed on September 7 and made landfall on Luzon Island in the Philippines with a maximum wind speed of approximately 110 knots before passing around 100 km south of Hong Kong. According to reporting by the Hong Kong Observatory, extensive circulation and fierce winds associated with Mangkhut on September 16 triggered record storm surges in many places and caused severe flooding in many low-lying coastal areas of Hong Kong, despite the event's temporal proximity to the occurrence of local neap tides.

Notice (11th April, 2019)
Figure 11 and 12 were found to be those for the year 2017. On 10th April 2019, TCC replaced these figures to the correct ones for 2018. Sorry for the inconvenience.

1 Here, a TC is defined as a tropical cyclone with a maximum sustained wind speed of 34 knots or more.

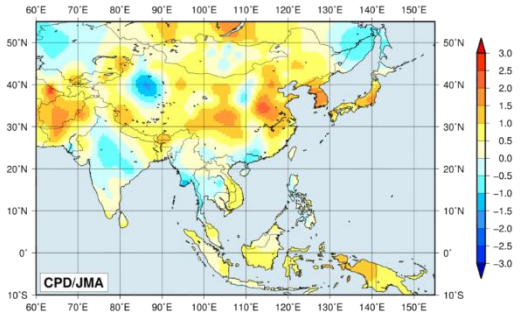

Figure 11 Four-month mean temperature anomalies (°C) from June to September 2018

The base period for normal is 1981 – 2010. Note that the data in Afghanistan, Bhutan, Cambodia, Kazakhstan, Nepal, North Korea, Papua New Guinea, Sri Lanka and Vietnam are interpolated due to the lack of CLIMAT report or climatological normal.

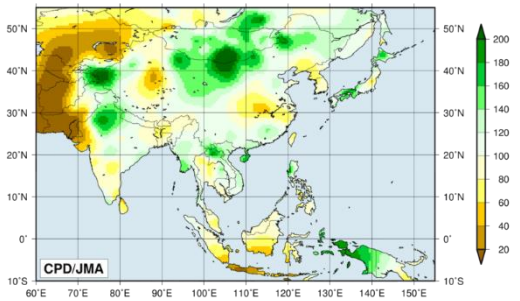

Figure 12 Four-month precipitation ratios (%) from June to September 2018

The base period for normal is 1981 – 2010. Note that the data in Afghanistan, Bhutan, Cambodia, Kazakhstan, Nepal, North Korea, Papua New Guinea, Sri Lanka and Vietnam are interpolated due to the lack of CLIMAT report or climatological normal.

Table 1 Tropical cyclones forming over the western North Pacific up to September 2018

Number ID	Name	Date (UTC)	Category[1)]	Maxumum wind[2)] (knots)
T1801	Bolaven	1/3–1/4	TS	35
T1802	Sanba	2/11–2/13	TS	35
T1803	Jelawat	3/25–4/1	TY	105
T1804	Ewiniar	6/5–6/8	TS	40
T1805	Maliksi	6/8–6/11	STS	60
T1806	Gaemi	6/15–6/17	TS	45
T1807	Prapiroon	6/29–7/4	TY	65
T1808	Maria	7/4–7/11	TY	105
T1809	Son-Tinh	7/17–7/19	TS	40
T1810	Ampil	7/18–7/23	STS	50
T1811	Wukong	7/23–7/27	STS	50
T1812[3)]	Jongdari	7/24–8/3	TY	75
T1813	Shanshan	8/3–8/10	TY	70
T1814	Yagi	8/4–8/13	TS	40
T1815	Leepi	8/11–8/15	STS	50
T1816	Bebinca	8/13–8/17	TS	45
T1817[4)]	Hector	8/13–8/15	TS	40
T1818	Rumbia	8/15–8/18	TS	45
T1819	Soulik	8/16–8/24	TY	85
T1820	Cimaron	8/18–8/24	TY	60
T1821	Jebi	8/27–9/4	TY	105
T1822	Mangkhut	9/7–9/17	TY	110
T1823	Barijat	9/11–9/13	TS	40
T1824[5)]	Trami	9/21–10/1	TY	105
T1825[5)]	Kong-Rey	9/29–10/6	TY	105

Note: Based on information from the RSMC Tokyo-Typhoon Center.
1) Intensity classification for tropical cyclones
TS: tropical storm, STS: severe tropical storm, TY: typhoon
2) Estimated maximum 10-minute mean wind.
3) Date of Typhoon Jongdari includes the period that it was temporally degraded from TC.
4) Typhoon Hector crossed the International Dateline from the East Pacific basin, the date indicates the period that it located in the West Pacific basin.
5) Based on early analysis data, not best track.

3. Monsoon activity and atmospheric circulation

Convective activity (inferred from OLR) averaged for June – September 2018 was enhanced from the Philippines to the Mariana Islands and over northwestern India, and was suppressed from the Indian Ocean to the western part of the Maritime Continent (Figure 13). OLR index data (Table 2) indicate that the overall activity of the Asian summer monsoon (represented by the SAMOI (A) index) was above normal from June to August and was below normal in May and from September to October. The active convection area was shifted northward (SAMOI (N) index) and eastward (SAMOI (W) index) of its normal position from June to August. Strengthened convective activity around the Philippines (Figure 14) was observed several times between June and August, indicating an active Southeast Asian monsoon.

In the upper troposphere (Figure 15 (a)), northeastward extension of the Tibetan High was stronger than normal and anticyclonic circulation anomalies straddling the equator were seen from Southeast Asia to the tropical western Pacific. In the lower troposphere (Figure 15 (b)), cyclonic circulation anomalies were seen from the northern part of the South China Sea to the seas east of the Philippines, indicating a stronger-than-normal monsoon trough over Southeast Asia. Surface westerly winds (Figure 16) were stronger than normal from the southern part of the South China Sea to the Mariana Islands. Zonal wind shear between the upper and lower troposphere over the North Indian Ocean and southern Asia (Figure 17) was stronger than normal from June to August.

(Section 1 and 2: Kenji Kamiguchi, 3: Hiroki Togawa, Climate Prediction Division)

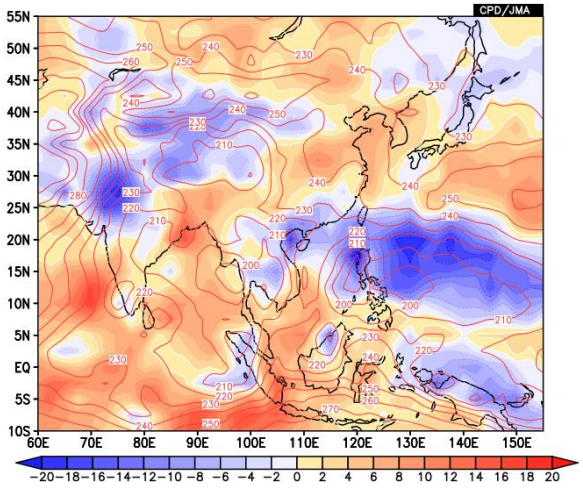

Figure 13 Four-month mean OLR and its anomaly for June–September 2018

The contours indicate OLR at intervals of 10 W/m^2, and the color shading denotes OLR anomalies from the normal (i.e., the 1981–2010 average). Negative (cold color) and positive (warm color) OLR anomalies show enhanced and suppressed convection compared to the normal, respectively. Original data are provided by NOAA.

Table 2 Summer Asian Monsoon OLR Index (SAMOI) values observed from May to October 2018

Asian summer monsoon OLR indices (SAMOI) are derived from OLR anomalies from May to October. SAMOI (A), (N) and (W) indicate the overall activity of the Asian summer monsoon, its northward shift and its westward shift, respectively. SAMOI definitions are as follows: SAMOI (A) = (-1) × (W + E); SAMOI (N) = S – N; SAMOI (W) = E – W. W, E, N and S indicate area-averaged OLR anomalies for the respective regions shown in the figure on the right normalized by their standard deviations.

	Summer Asian Monsoon OLR Index (SAMOI)		
	SAMOI (A): Activity	SAMOI (N): Northward-shift	SAMOI (W): Westward-shift
May 2018	-0.7	-2.2	1.6
Jun. 2018	0.8	1.8	-0.7
Jul. 2018	1.0	0.6	-1.3
Aug. 2018	0.6	2.1	-0.3
Sep. 2018	-1.4	-0.1	-2.0
Oct. 2018	-1.5	-1.0	1.4

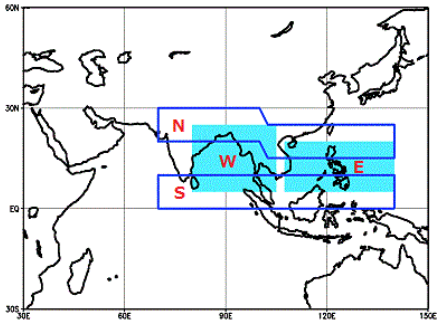

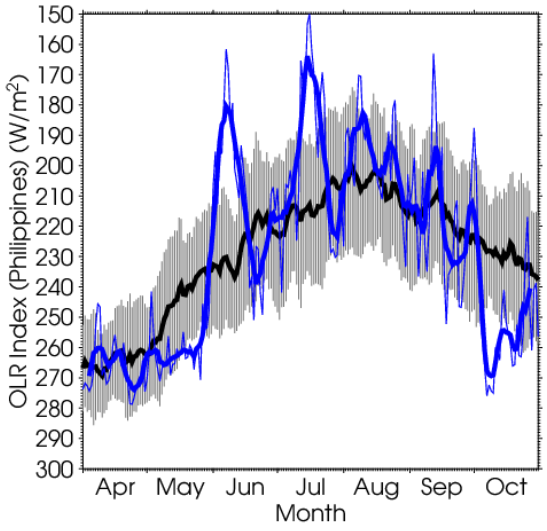

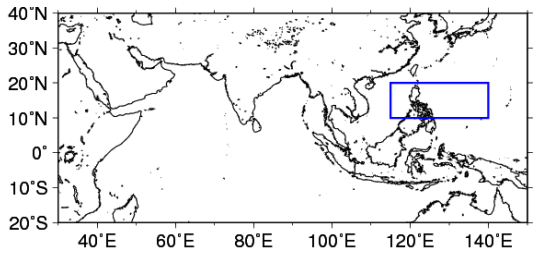

Figure 14 Time-series representation of OLR (W/m^2) averaged over the Philippines (shown by the rectangle on the right: 10°N - 20°N, 115°E - 140°E)

The OLR index is calculated after Wang and Fan (1999). The thick and thin blue lines indicate seven-day running mean and daily mean values, respectively. The black line denotes the normal (i.e., the 1981 - 2010 average), and the gray shading shows the range of the standard deviation calculated for the time period of the normal.

(a)

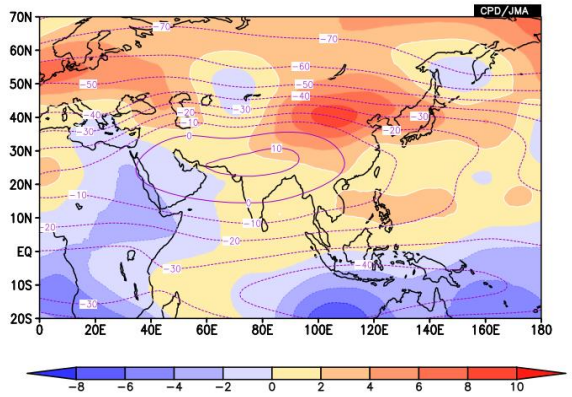

(b)

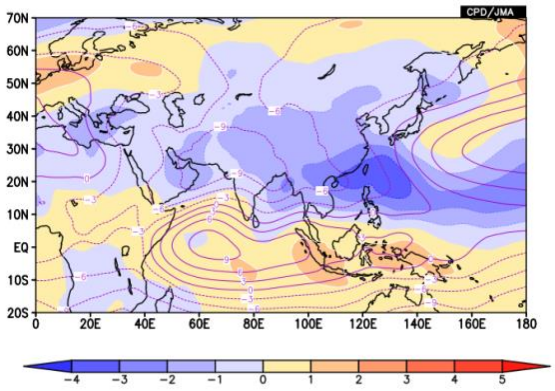

Figure 15 Four-month mean (a) 200-hPa and (b) 850-hPa stream function (contour) and its anomaly (color shading) for June–September 2018

Contour intervals are (a) 10 × 10^6 m^2/s and (b) 4 × 10^6 m^2/s. Warm (cold) shading denotes anticyclonic (cyclonic) circulation anomalies in the Northern Hemisphere, and vice-versa in the Southern Hemisphere. The base period for the normal is 1981 – 2010.

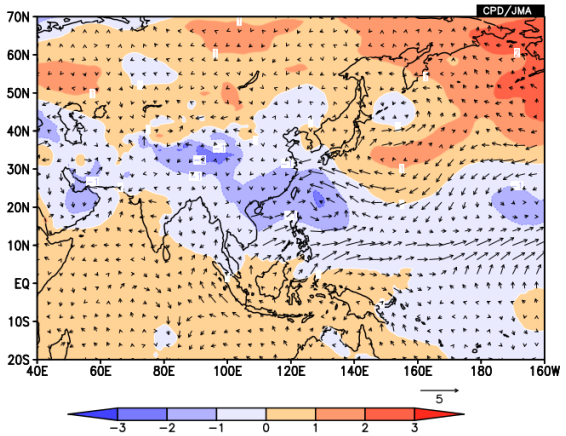

Figure 16 Sea level pressure anomaly (shade) and surface wind vector anomaly (vectors) for June–September 2018.

The shade shows sea level pressure anomalies at intervals of 1 hPa. The base period for the normal is 1981 – 2010.

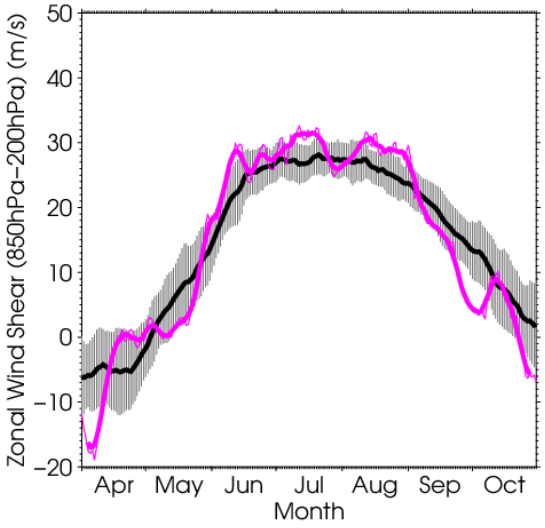

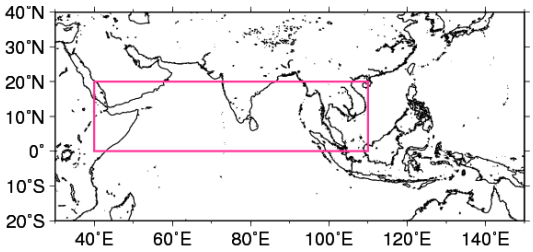

Figure 17 Time-series representation of the zonal wind shear index between 200-hPa and 850-hPa averaged over the North Indian Ocean and southern Asia (the region enclosed by the pink rectangle in the right figure: equator – 20°N, 40°E – 110°E)
The zonal wind shear index is calculated after Webster and Yang (1992). The thick and thin pink lines indicate seven-day running mean and daily mean values, respectively. The black line denotes the normal (i.e., the 1981 – 2010 average), and the gray shading shows the range of the standard deviation calculated for the time period of the normal.

References

Wang, B., and Z. Fan. 1999. Choice of South Asian summer monsoon indices. Bulletin of the American Meteorological Society 80:629–638, http://dx.doi.org/10.1175/1520-0477(1999)080<0629:COSASM>2.0.CO;2.

Webster, P. J. and S. Yang, 1992: Monsoon and ENSO: Selectively interactive systems. *Quart. J. Roy. Meteor. Soc.*, **118**, 877 – 926.

Status of the Antarctic Ozone Hole in 2018

The size of the Antarctic ozone hole in 2018 has exceeded the most recent decadal average due to very cold stratospheric conditions. However, a statistically significant decrease in its maximum size since 2000 is observed.

Since the early 1980s, the Antarctic ozone hole has appeared every year in austral spring with a peak in September or early October. It is generally defined as the area in which the total ozone column value is below 220 m atm-cm.

According to JMA analysis based on data from the Ozone Monitoring Instrument (OMI) on the Aura platform, the Antarctic ozone hole in 2018 appeared in mid-August, expanded rapidly from late August onward, and has developed to become larger than the most recent decadal average (Figure 18, upper left). Its maximum size for the year (observed on 20 September) was 24.6 million square kilometers (see the upper-right panel in Figure 18), which is 1.8 times as large as the Antarctic Continent itself. In 2018, the polar vortex over Antarctica was stable and large, and the stratospheric temperature was much lower than the most recent decadal average after mid-July. This resulted in increased formation of polar stratospheric clouds (PSCs), which play an important role in ozone destruction, and may have contributed to the expanded scale of the year's ozone hole. However, a statistically significant decrease in the maximum size of the Antarctic ozone hole since 2000 has been identified. The report titled *WMO/UNEP Scientific Assessment of Ozone Depletion: 2018* detailed that the hole is expected to close gradually, with spring-time total column ozone in the 2060s returning to 1980 values.

The ozone layer acts as a shield against ultraviolet radiation, which can cause skin cancer. The ozone hole was first recognized in the early 1980s and reached its maximum size of 29.6 million square kilometers in 2000. The Antarctic ozone hole significantly affects summer climatic conditions on the surface of the Southern Hemisphere according to the recent assessment.

(Takanori Matsumoto, Ozone Layer Monitoring Center)